

Dynamics of Single Rising Bubbles in Neutrally Buoyant Liquid-Solid Suspensions

Nasim Hooshyar,¹ J. Ruud van Ommen,¹ Peter J. Hamersma,¹ Sankaran Sundaresan,² and Robert F. Mudde^{1,*}

¹*Department of Chemical Engineering, Delft University of Technology, Julianalaan 136, 2628 BL Delft, The Netherlands*

²*Chemical Engineering Department, Princeton University, Princeton, New Jersey 08543, USA*

(Received 24 October 2012; revised manuscript received 9 March 2013; published 11 June 2013)

We experimentally investigate the effect of particles on the dynamics of a gas bubble rising in a liquid-solid suspension while the particles are equally sized and neutrally buoyant. Using the Stokes number as a universal scale, we show that when a bubble rises through a suspension characterized by a low Stokes number (in our case, small particles), it will hardly collide with the particles and will experience the suspension as a pseudoclear liquid. On the other hand, when the Stokes number is high (large particles), the high particle inertia leads to direct collisions with the bubble. In that case, Newton's collision rule applies, and direct exchange of momentum and energy between the bubble and the particles occurs. We present a simple theory that describes the underlying mechanism determining the terminal bubble velocity.

DOI: [10.1103/PhysRevLett.110.244501](https://doi.org/10.1103/PhysRevLett.110.244501)

PACS numbers: 47.55.D–

Bubbles, or other deformable particles, moving in clear liquids or liquid-solid mixtures are important in numerous fields such as oil and gas production [1,2], food processing [3], biotechnology [4], algae production [5] and the flow of blood inside the human body [6]. The shape, oscillation, path, and velocity of gas bubbles rising in clear liquids have been studied extensively [7–10]. In contrast, there have been very few studies that focus on the dynamics of gas bubbles in liquid-solid suspensions. Fan and Tsuchiya [7] investigated the bubble wake in liquid-solid suspensions and showed that the wake size is sensitive to the extent of the disturbance in the liquid flow caused by the presence of the particles. Vera *et al.* [11] studied the instabilities of gas bubbles in a liquid-fluidized bed and described the series of instabilities induced by a downward liquid flow through a foam of bubbles. Some researchers have proposed correlations for bubble rise velocity in liquid-solid suspensions [12]. However, the nature of interactions between a rising bubble and particles in a liquid-solid suspension, a rather basic problem in physics, has not received close scrutiny.

The objective of the present research is to study the influence of particles on the average rise velocity of a single gas bubble in a suspension of spherical particles. In general, the density of the particles will differ from that of the liquid, and the particles will sediment or rise in the liquid as a result of the gravitational and buoyancy forces. Thus, the rising gas bubble will interact with sedimenting or rising particles. In the present study, we simplify the problem by considering only neutrally buoyant suspensions [13]. We classify the system in terms of the ratio between the Stokes relaxation time of the particles ($\tau_p = \rho_p d_s^2 / 18\mu$, with the particle density ρ_p , the solid diameter d_s , and the liquid viscosity μ) and the characteristic time of the rising bubble ($\tau_b = d_b / v_b$, with the bubble diameter d_b and the bubble velocity v_b), $St = \tau_p / \tau_b$ [14]. We experimentally show that the Stokes number (St) is the

most important parameter for understanding the bubble dynamics with a regime transition from the direct to indirect particle interaction around $St = 1$.

In this Letter, we report detailed experiments on the terminal velocity of a single bubble rising through a neutrally buoyant liquid-particle suspension. Experiments were performed in a rectangular column [Fig. 1(a)]. The column (cross section 50×50 mm, height 200 mm) was filled with a water-glycerol mixture having the same density as the suspended, spherical polystyrene particles ($d_s = 78$ and $587 \mu\text{m}$, 2.0 and 4.0 mm). The liquid mixture density was 1054 kg/m^3 , slightly varying with the different particles used. An air bubble with an equivalent diameter of about 3.0 mm was injected via a needle with an i.d. of 0.8 mm located at the bottom center of the column. The flow behavior of the rising bubble and the surrounding particles in suspensions containing particles at very low

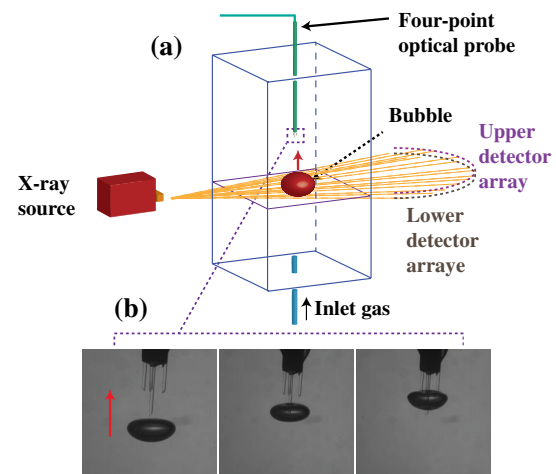


FIG. 1 (color online). Gas bubble formation, motion and detection in water-glycerol-polystyrene mixture. (a) Schematic of the setup, (b) sequences of a single rising bubble being pierced with the four-point optical probe.

volume fractions was recorded using a high-speed camera (1000 fps). At higher particle volume fractions where the system is opaque, we obtained information on the bubble motion and shape by using a four-point optical probe [Fig. 1(b)] [15]. For large particle sizes (2.0 and 4.0 mm), where the optical probe could not be used reliably, the bubble characteristics were measured using fast x-ray densitometry [16]. The consistency of the measurements with different techniques has been ascertained (see Supplemental Material [17]).

The motion of a single rising bubble in a water-glycerol mixture at $25 \pm 0.5^\circ\text{C}$ was captured in the series of images shown in Figs. 2(a)–2(d). We categorize the systems in terms of the Stokes number. Figure 2(a) shows that for the system with $78\ \mu\text{m}$ particles ($St = 0.016 \ll 1$), the particles remained virtually on the streamlines of the liquid flowing around the bubble (see Supplemental Material [17], Movie 1) and the mixture of liquid and particles behaved as a pseudoclear liquid. The motion of the bubble

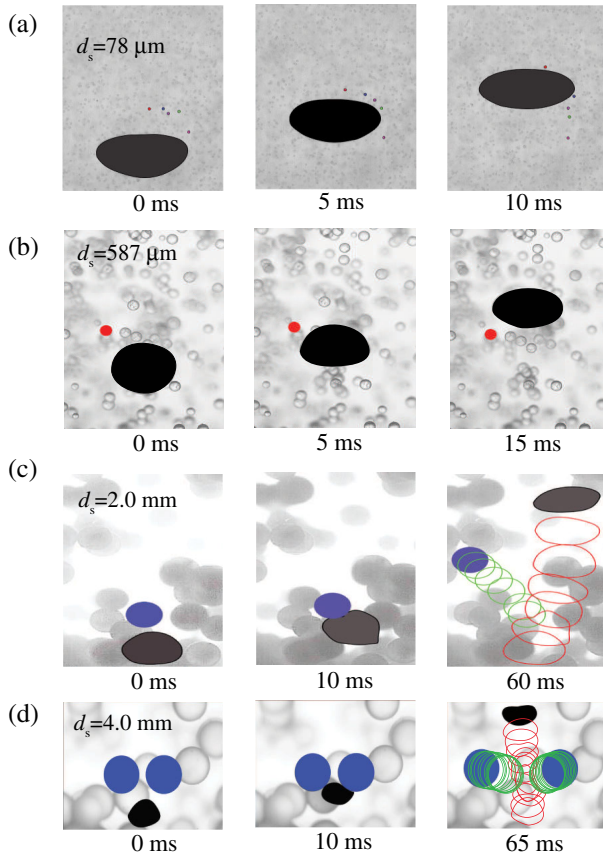


FIG. 2 (color online). Gas bubble motion in water-glycerol-polystyrene mixture: (a) and (b) 78 and $587\ \mu\text{m}$ particles with $St \ll 1$ remain on the streamline of the liquid and do not collide on the bubble surface, (c) $2.0\ \text{mm}$ particle with $St \gg 1$ and $d_s < d_b$ collides with the bubble and changes the bubble's direction of motion, and (d) $4.0\ \text{mm}$ particles with $St \gg 1$ and $d_s > d_b$ encounter the rising bubble. For more details, see Supplemental Material [17], Movies 1–3.

could be described by replacing the suspension with a clear liquid having the same viscosity and surface tension as the liquid-solid suspension. The influence of the suspended particles was merely to increase the viscosity. The same is true for suspended particles of $587\ \mu\text{m}$ diameter ($St = 0.88$). Figure 2(c) shows that with $2.0\ \text{mm}$ particles ($St = 10.1 \gg 1$, but the particle size still smaller than the bubble size), the particles collided with the bubble (see Supplemental Material [17], Movie 2). With $4.0\ \text{mm}$ particles ($St = 41.2$, and the particles larger than the bubble) collisions between the particles and the rising bubble were very prominent [see Fig. 2(d) and Supplemental Material [17], Movie 3]. Clearly, above a critical value of the St number, the particles no longer migrate with the liquid around the bubble but collide with the bubble and change its direction of motion.

Figure 3 illustrates that the bubble rise velocity decreases with an increase in the particle volume fraction for all St and that the extent of reduction depends on St . The observed reduction in the bubble velocity for $St \ll 1$ is to be expected. As the small particles do not directly collide with the bubble, their effect is felt as an (apparent) increase in the viscosity of the mixture. A commonly used model for the effective viscosity, μ_{eff} , of a suspension of small particles ($St \ll 1$) capturing the increase in μ_{eff} with increasing solids volume fraction, C_s , is [18]:

$$\frac{\mu_{\text{eff}}}{\mu_0} = (1 - C_s/C_m)^{-n}, \quad (1)$$

where μ_0 is the viscosity of solids-free liquid and C_m is the random close packing concentration for a given system. We set $n = 2.5C_m$ so that at small C_s values one recovers the Einstein equation for the viscosity of a dilute suspension of solids in a liquid [19]: $\mu_{\text{eff}}/\mu_0 = (1 + 2.5C_s)$.

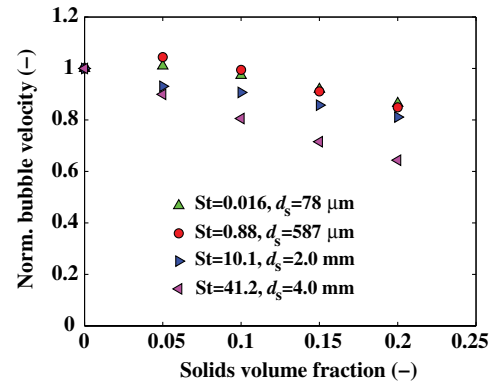


FIG. 3 (color online). Effect of St on the bubble velocity: the superficial gas velocity. The results of systems with 78 and $587\ \mu\text{m}$ particles are from measurements with the four-point optical probe and are the average of the bubble velocity values in different vertical elevations. The bubble rise velocities in suspensions with 2.0 and $4.0\ \text{mm}$ particles are the results of measurements with the x-ray densitometry. The velocity values are normalized to the velocity obtained in clear liquid.

The viscosity and the surface tension of suspensions of 78 μm particles were measured. The surface tension was found to be independent of the solids concentration and had an average value of $\sigma = 66.92 \pm 0.20$ mN/m. For the highest solids fraction examined in this study, the apparent viscosity was almost double that of the suspending liquid. Equation (1) with $C_m = 0.65$ [20] captures the data satisfactorily. Using a force balance between the drag and buoyancy for the single rising bubble yields the following expression for the bubble velocity:

$$v_b = \sqrt{\frac{2(\rho_{\text{liq}} - \rho_g)V_B g}{C_D A_{\perp} \rho_{\text{liq}}}}, \quad (2)$$

where V_B is the bubble volume, ρ_{liq} the liquid density, ρ_g is the gas density and C_D and A_{\perp} are the drag coefficient and the frontal bubble area. We calculate the drag coefficient with the expression of Tomiyama [21] for contaminated systems; all other parameters are known. The calculated bubble velocities as a function for different particle velocities are shown in Fig. 4, along with the experimental data. At low particle volume fractions where the drag force is dominated by surface tension effects, there is little change in the rise velocity with C_s . At somewhat higher particle loading levels and, hence, higher viscosities, the viscous effect becomes more important than surface tension and the bubble velocity begins to decrease with increasing particle volume fraction. In order to ascertain that the increased viscosity is the reason for the reduced bubble rise velocity at $\text{St} \ll 1$, we performed bubble rise experiments using a clear liquid having the same viscosity as the suspension by adjusting the glycerol fraction. Figure 4 confirms that for $\text{St} \ll 1$, the rise velocity of the bubble in the presence of particles can be found by replacing the mixture with a clear liquid having the same viscosity and

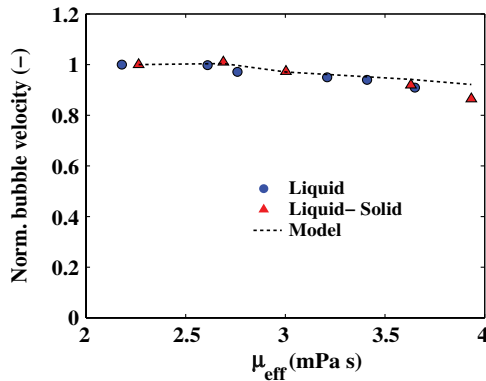


FIG. 4 (color online). Influence of the effective viscosity on the bubble velocity. A single rising bubble in a neutrally buoyant suspension of 78 μm polystyrene particles is found to behave the same as that in clear liquid with the same effective viscosity. The velocity values are normalized to the velocities at $\mu = 2.2$ mPa s. The dashed line corresponds to Eq. (2).

surface tension as the suspension. As can be seen in Fig. 4, the bubble rise velocity seems to go up from $\mu_{\text{eff}} = 2.3$ to 2.7 mPa s and in Fig. 3 at $\text{St} \ll 1$ from $C_s = 0$ to 5%. The velocity again drops with a further increase in the μ_{eff} and C_s . This is due to the fact that at low μ_{eff} the bubble follows a zigzag path (see Fig. 3 in the Supplemental Material [17]). With an increase in the μ_{eff} , the bubble path becomes slightly tighter and, therefore, the bubble travels vertically a longer height in a given time than for the 0% solid loading. With further increase in particle volume fraction the bubble velocity decreases as a result of the increase in the apparent viscosity.

Particles with a higher inertia, i.e., $\text{St} \gg 1$, do literally collide with a bubble. Figures 2(c) (Supplemental Material [17], Movie 2) and 2(d) (Supplemental Material [17], Movie 3) are examples of such collisions. In the first phase of the collision, the bubble slows down and gets deformed, while the particle gains momentum. In the second phase, the particle and bubble separate again; the bubble will regain its shape, but will have lost energy. We use a simple energy conservation argument to estimate the energy transferred from the bubble to the particle. The deformation of the bubble increases the bubble surface area. The associated increase in surface energy, $\Delta E_{\sigma} = \sigma \Delta A$ (where σ is the surface tension and ΔA is the change of surface area) goes at the expense of the kinetic energy of the bubble [22]. For the latter we take $m_v v_b^2/2$ (where m_v is the virtual mass of the bubble). During the collision, a portion of the deformation energy is transferred to the particle, while the remainder is dissipated as heat. The bubble will continue to migrate with a reduced kinetic energy: $m_v v_{\text{ac}}^2/2 = m_v v_{\text{bc}}^2/2 - \sigma \Delta A$ (with v_{bc} the bubble velocity just before collision and v_{ac} just after collision).

Subsequently, the bubble will accelerate in clear liquid due to the buoyancy force until it collides with the next particle and the cycle repeats. The accelerating part is governed by Newton's equation of motion: $m_v dv_b/dt = F_B - C_D A_{\perp} (\rho_{\text{liq}} v_b^2/2)$ with $m_v = \rho_{\text{liq}} V_B/2$, $F_B = (\rho_{\text{liq}} - \rho_g) V_B g$. For constant C_D the equation of motion is readily solved, giving the bubble's position and velocity as a function of time.

The bubble will travel on average a mean free path, λ_{mf} , between two successive collisions which are modeled as instantaneous events. We get the bubble travel time between two successive collisions from the sequence: (i) collision, $v_{\text{bc}}(i) \rightarrow v_{\text{ac}}(i)$; (ii) acceleration over one mean free path, $v_{\text{ac}}(i) \rightarrow v_{\text{bc}}(i+1)$ in a duration $\Delta \tau_{\text{mf}}$. In a steady state, the bubble will acquire such a velocity that $v_{\text{bc}}(i) = v_{\text{bc}}(i+1)$ with a time $\Delta \tau_{\text{mf}}$ between collision (for more detail see Fig. 8 in the Supplemental Material [17]). By solving the trajectory for this condition, we find the average rise velocity of the bubble:

$$\langle v \rangle = \frac{\lambda_{\text{mf}}}{\Delta \tau_{\text{mf}}}. \quad (3)$$

The mean free path is a function of the solids number density, n_p , and the particle and bubble diameter d_p and d_b , respectively:

$$\lambda_{mf} = \left[\sqrt{2} \pi n_p \left(\frac{d_p}{2} + \frac{d_b}{2} \right)^2 \right]^{-1}. \quad (4)$$

This description should hold when the mean free path is large compared to the particle and bubble size. As the 2.0 and 4.0 mm particles are of the same size as the bubbles, we use the bubble size as the characteristic length to define a Knudsen number: $Kn \equiv \lambda_{mf}/d_b$.

We argue that for Kn larger than one, the above reasoning should give a reasonable estimate of the bubble rise velocity. The mean free path for the 4.0 mm particles varies from 12.3 to 3.08 mm, giving $Kn \geq 1$. From the movies of the collisions [see Supplemental Material [17], Movie 3 and Fig. 2(d)], we estimated that the bubble deforms to an ellipsoid with a short axis of 2.0 mm and a long axis of 3.67 mm. Therefore, the surface energy increases from 1.92×10^{-6} J to 2.12×10^{-6} J, ignoring dynamic effects (e.g., rearrangement of contaminant molecules at the surface) as a first-order approximation. The 2.0×10^{-7} J enhancement in the surface energy leads to a 2.0×10^{-7} J reduction in the kinetic energy. Assuming the experimentally observed terminal velocity of 0.25 m/s at the velocity before the collision, this translates into a velocity reduction of 40% upon collision: $v_{ac}(i) = 0.6v_{bc}(i)$; see Sec. 4 of the Supplemental Material [17] for a more elaborate discussion. This number was used to analyze the collision-acceleration trajectory of a bubble. The dashed line in Fig. 5 shows the outcome of such an analysis. The line describes the experimental points very well. We performed a similar analysis for the 2.0 mm particles as well, where Kn was found to be order one or smaller and multiparticle collisions may become important, rendering estimation of the energy loss very difficult. From the movies, it was estimated that the increase in bubble surface area associated with its deformation during collision with a single particle was not more than 1 mm^2 . An increase in surface area of 1 mm^2 is equivalent to a change in kinetic energy of 6.7×10^{-8} J. Based on the virtual mass of the bubble and a velocity before collision $v_{bc}(i) = 0.25 \text{ m/s}$, it then follows that the velocity after collision $v_{ac}(i) = 0.84v_{bc}(i)$; when this was combined with the above mean free path analysis, the average rise velocity was under-predicted. The solid line drawn in Fig. 5 matches the 2.0 mm data if we set $v_{ac}(i) = 0.95v_{bc}(i)$, which is equivalent to an increase in surface area by 0.34 mm^2 . In spite of the difficulty in estimating the energy loss in a collision, it is encouraging that a model based on energy loss captures the experimental data.

Our study highlights that the microscopic behavior of a gas, liquid, and solid system changes with increasing St . When $St \ll 1$, the particles do not collide with the bubble and the bubble rises as in a clear liquid having the same

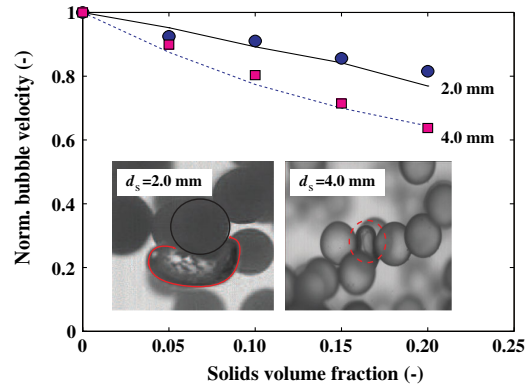


FIG. 5 (color online). Influence of 2.0 and 4.0 mm particles on the bubble velocity. The solid and dashed lines correspond to the estimated values for the average bubble velocity and the symbols correspond to the experimental results measured by x-ray densitometry; inset, 2.0 mm case: the red line around the bubble shows its deformation and in the 4.0 mm case: the red dashed line on the image denotes the squeezed bubble.

viscosity and surface tension as the suspension. Collisions between particles and bubble, which occur at $St \gg 1$, lead to bubble deformation and a decrease in bubble velocity. When $Kn \geq 1$, a mean free path analysis based on repeated collision between a single particle and the bubble adequately captures the effect of particles on the average bubble rise velocity. Although the average rise velocity of the bubble decreases with increasing solids volume fraction at both small and large St , the underlying microscopic events leading to the observed macroscopic behavior differ significantly. For example, one can ask how the rate of transfer of a species between the gas and the suspension is influenced by the particles. Lower rise velocity usually implies a lower mass transfer coefficient [23], which is likely to be the outcome for suspensions with $St \ll 1$. In contrast, repeated bubble deformation that occurs when $St \gg 1$ may enhance interphase mass transfer. Such questions remain to be explored. It is crucial to understand this difference to properly interpret and model the dynamics of bubble rise in technological as well as natural contexts where the particle-bubble interaction is further complicated by gravitational settling of nonneutrally buoyant particles.

*r.f.mudde@tudelft.nl

- [1] M. Al-Asimi, G. Butler, G. Brown, A. Hartog, T. Clancy, C. Cosad, J. Fitzgerald, J. Navarro, A. Gabb, J. Ingham, S. Kimminau, J. Smith, and K. Stephenson, *Oilfield review/Schlumberger* **14**, 14 (2003).
- [2] S. Guet and G. Ooms, *Annu. Rev. Fluid Mech.* **38**, 225 (2006).
- [3] B. R. Pinzer, A. Medebach, H. J. Limbach, C. Dubois, M. Stampanoni, and M. Schneebeli, *Soft Matter* **8**, 4584 (2012).
- [4] F. Garcia-Ochoa and E. Gomez, *Biotechnology advances* **27**, 153 (2009).

- [5] L. Rodolfi, G. C. Zittelli, N. Bassi, G. Padovani, N. Biondi, G. Bonini, and M. R. Tredici, *Biotechnol. Bioeng.* **102**, 100 (2009).
- [6] J. K. W. Chesnutt and J. S. Marshall, *Microvasc. Res.* **78**, 301 (2009).
- [7] L.-S. Fan and K. Tsuchiya, *Bubble Wake Dynamics in Liquids and Liquid-Solid Suspensions* (Butterworth-Heinemann, Stoneham, MA, 1990).
- [8] N. Z. Handzy and A. Belmonte, *Phys. Rev. Lett.* **92**, 124501 (2004).
- [9] G. Mougin and J. Magnaudet, *Phys. Rev. Lett.* **88**, 014502 (2001).
- [10] W. L. Shew and J.-F. Pinton, *Phys. Rev. Lett.* **97**, 144508 (2006).
- [11] M. U. Vera, A. Saint-Jalmes, and D. J. Durian, *Phys. Rev. Lett.* **84**, 3001 (2000).
- [12] X. Luo, J. Zhang, K. Tsuchiya, and L.-S. Fan, *Chem. Eng. Sci.* **52**, 3693 (1997).
- [13] N. T. Ouellette, P. J. J. O'Malley, and J. P. Gollub, *Phys. Rev. Lett.* **101**, 174504 (2008).
- [14] Y. Tagawa, J. M. Mercado, V. N. Prakash, E. Calzavarini, C. Sun, and D. Lohse, *J. Fluid Mech.* **693**, 201 (2012).
- [15] R. F. Mudde and T. Saito, *J. Fluid Mech.* **437**, 203 (2001).
- [16] R. F. Mudde, *Powder Technol.* **199**, 55 (2010).
- [17] See Supplemental Material at <http://link.aps.org/supplemental/10.1103/PhysRevLett.110.244501> for a more in depth description of the methods used and for a graphical illustration of finding, in case of the solids with a higher Stokes number, the bubble velocity just prior to the next collision from the velocity just after the previous collision.
- [18] I. M. Krieger, *Adv. Colloid Interface Sci.* **3**, 111 (1972).
- [19] A. Einstein, *Ann. Phys. (Berlin)* **324**, 289 (1906).
- [20] J.-P. Matas, J. Morris, and E. Guazzelli, *Phys. Rev. Lett.* **90**, 014501 (2003).
- [21] A. Tomiyama, I. Kataoka, I. Zun, and T. Sakaguchi, *JSME Int J. Ser. B.* **41**, 472 (1998).
- [22] R. Zenit and D. Legendre, *Phys. Fluids* **21**, 083306 (2009).
- [23] R. Clift, J. R. Grace, and M. E. Weber (Academic Press, New York, 1978).